# Distributed Sensing in Capacitive Conductive Composites

Edward L. White, Michelle C. Yuen, and Rebecca K. Kramer
School of Mechanical Engineering
Purdue University
West Lafayette, IN, USA
rebeccakramer@purdue.edu

***Abstract*—In this paper, we describe a capacitance-based strain field sensor. The device is interrogated at a single location, and uses multiple excitation frequencies to resolve the spatial distribution of strain. The system we model is representative of a capacitor composed of a graphite-based conductive elastomer composite in a silicone binder with a silicone dielectric layer. We utilize an artificial neural network to reconstruct the strain based on the magnitude of the measured impedance. Our analysis uses finite element simulation to demonstrate the concept in a one-dimensional application. We demonstrate that multiple elements can be interrogated using a single electrical interface, reducing the complexity of high deformation sensor arrays.**

***Keywords—distributed sensing, dielectric elastomer sensors, high-deformation sensing, capacitive sensor impedance***

## I. INTRODUCTION

Measuring large strains and deformations is required in many applications involving soft bodies [1], including both soft robot and wearable applications [2]. In traditional robots and rigid mechanisms, deformations are concentrated at joints. In soft-bodied systems, however, deformations are distributed throughout the structure, requiring that sensors likewise be distributed. However, distributing sensors poses two challenges. First, it increases the total number of sensors which must be fabricated and integrated. Second, it increases the total number of interfaces between the sensors and the associated signal conditioning electronics. In many cases, these two requirements work against the goal of the soft system, which is to maintain high deformations and low elastic modulus. Furthermore, increasing the number of devices and interfaces can reduce the overall reliability of the soft system.

Instead of a traditional paradigm where a single sensor is used to measure strain at a single point, we demonstrate a method to measure strain at multiple locations with a single physical device. This method allows us to reduce the total number of sensors which must be fabricated, and consequently drives down the total number of interface electrodes. As noted by previous authors, a one-dimensional capacitive sensor with finite electrode resistance can be modeled as an RC network [3,4]. By adjusting the excitation frequency of the sensor, we are able to control the distribution of the electric field within the equivalent RC network, which in turn allows us to control the spatial sensitivity of the device. Therefore, by exciting the sensor at multiple frequencies and measuring the impedance, we can uniquely reconstruct the strain at multiple locations along the length of the sensor. Previously, researchers have constructed a keyboard by using multiple frequencies to measure deformation due to pressure at different locations on a two dimensional monolithic substrate [5]. Additionally, a single interface has been used to interrogate multiple capacitive strain sensor elements connected in series [6]. Our work extends these previous examples by demonstrating how continuous values of strain can be measured in multiple elements along the length of a single sensor body.

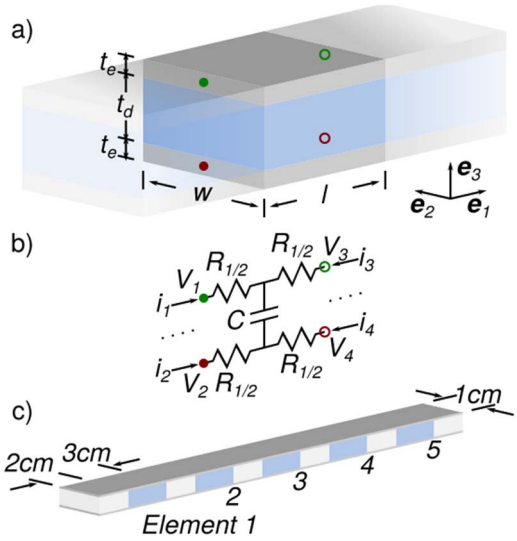


Fig. 1. Simulation representation. a) A 1-D electromechanical element. The length of the element is *l*, the width is *w*, and the electrode and dielectric thicknesses are $t_e$ and $t_d$, respectively. Note the directions of the Cartesian coordinate system **e**. b) The corresponding electrical element of the mechanical element shown in a). Note that the red and green dots shown in a) and b) are shown in the same relative locations. c) The complete 5-element sensor. The deformable regions are shown in blue, while the reinforced mounting regions are shown in white.

## II. FINITE ELEMENT SIMULATION

### A. Model Development

The conductive elastomer composite sensors we discuss in this work are designed for applications with large deformations (>50% strain). To accurately capture these finite deformations, we used a Lagrangian mesh throughout our analysis, since a linear approximation was insufficient to capture the non-linear geometry of the sensor. Instead of solving for the complete electrical field around and within the sensor, we used a direct

978-1-5090-1012-7/17/$31.00 ©2017 IEEE

analysis technique to construct an element which represented both the resistance of the electrode and capacitance of the dielectric layer within a finite thickness slice of the sensor. The physical and electrical representations of a single element are shown in Fig. 1(a-b). The resistance, $R_{1/2}$, of the electrode element is defined by:

$$R_{1/2} = \rho(\epsilon)\frac{l}{2wt_e}$$

where $\rho(\epsilon)$ is the resistivity as a function of the strain, $l$ is the current length of the element, $w$ is the current width, and $t_e$ is the current thickness of the electrode. The subscript $_{1/2}$ indicates that the resistance only covers one half of the length of the element. The capacitance of the element is:

$$C = \varepsilon_0\varepsilon_r\frac{wl}{t_d}$$

where $\varepsilon_0$ is the permittivity of free space, $\varepsilon_r$ is the relative permittivity of the dielectric layer, and $t_d$ is the thickness of the dielectric. Assuming that the material is incompressible and isotropic, these equations become:

$$C = \varepsilon_0\varepsilon_r\frac{w_0 l_0(1+\epsilon)}{t_{d0}}$$

and

$$R_{1/2} = \rho(\epsilon)\frac{l_0(1+\epsilon)^2}{2w_0 t_{e0}}$$

where the $_0$ subscript denotes initial conditions. The governing equation of a single element is:

$$\begin{bmatrix} i_1 \\ i_2 \\ i_3 \\ i_4 \end{bmatrix} = \begin{bmatrix} a & b & c & b \\ b & a & b & c \\ c & b & a & b \\ b & c & b & a \end{bmatrix}\begin{bmatrix} V_1 \\ V_2 \\ V_3 \\ V_4 \end{bmatrix} \quad (1)$$

where:

$$a = \frac{1}{4}\frac{3Z_R + 2Z_C}{(Z_R + Z_C)Z_R}$$

$$b = -\frac{1}{4}\frac{1}{(Z_R + Z_C)}$$

$$c = -\frac{1}{4}\frac{Z_R + 2Z_C}{(Z_R + Z_C)Z_R}$$

where $Z_R = R_{1/2}$ and $Z_C = 1/(j\omega C)$ represent the complex impedances of the resistor and capacitor, respectively.

### B. *Physical Concept*

To demonstrate the concept of measuring strain at multiple points within a single sensor, we propose a five-element sensor as shown in Fig. 1(c). The sensor is composed of inextensible regions, shown as white segments, and stretchable regions, shown as blue segments. We intend to build this device from elastomer-based conductive composites, where expanded intercalated graphite is used as a conductive phase in the electrode material [7]. The notional dimensions used in the model are a width of 1cm, an inextensible segment length of 2cm and an extensible segment length of 3cm. We have found that a linear resistivity model of the form $\rho(\epsilon)=\rho_0+\rho_1\epsilon$ adequately captures the behavior of the conductive electrode material.

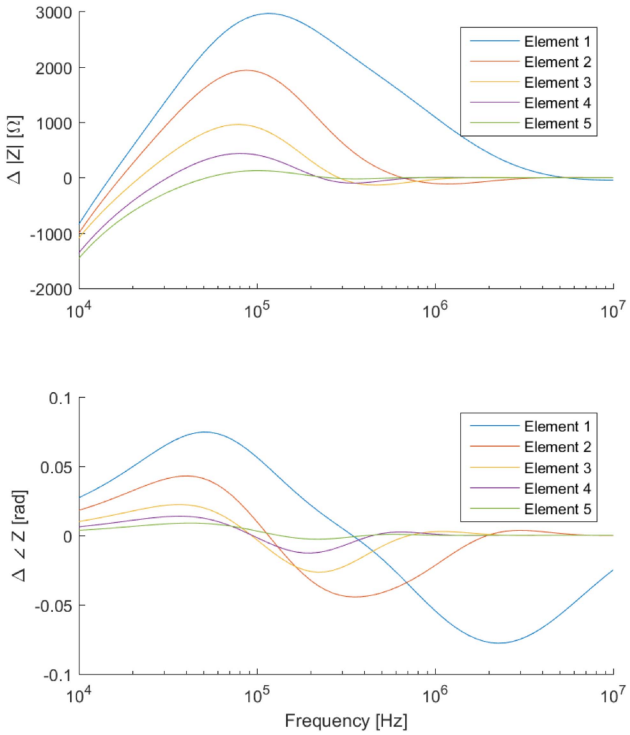


Fig. 2. Change in resistance (top) and capacitance (bottom) relative to baseline values when individual sensor elements are strained by 10%. Each strain is applied individually, i.e. the element 1 test applied a 10% strain to element 1, leaving all other elements unstrained.

We conducted a preliminary FEM study with the model to understand the sensitivity to strain of each element when deformed individually prior to applying simultaneous deformations. We applied a 10% strain to each element in turn and simulated the overall impedance of the resulting system, with the results shown in Fig. 2. The plot of impedance demonstrates several interesting effects. First, at the low frequency limit, strain in every element results in a similar change in impedance. Since at low excitation frequencies the field is approximately uniform along the length of the sensor, changes in impedance at any point will have similar impact as any other point. The differences between each element are due to the changes in resistivity. If the resistivity was unchanging, the changes in impedance would be identical. Second, at the high frequency limit, no change in impedance is observed for strain in any element. At high frequencies, any applied potential is shunted through the sensor in the immediate vicinity of the electrodes, and there is no potential between the upper and lower electrodes along the body of the sensor. Finally, we observe that within the range $f \in [10^4, 10^7]Hz$, applying the same strain to each element of the sensor produces different responses, with the element closest to the electrodes producing the largest response and the element furthest away producing the smallest response. Therefore, by probing the sensor across this frequency range, we can differentiate the strains at different elements within the sensor.

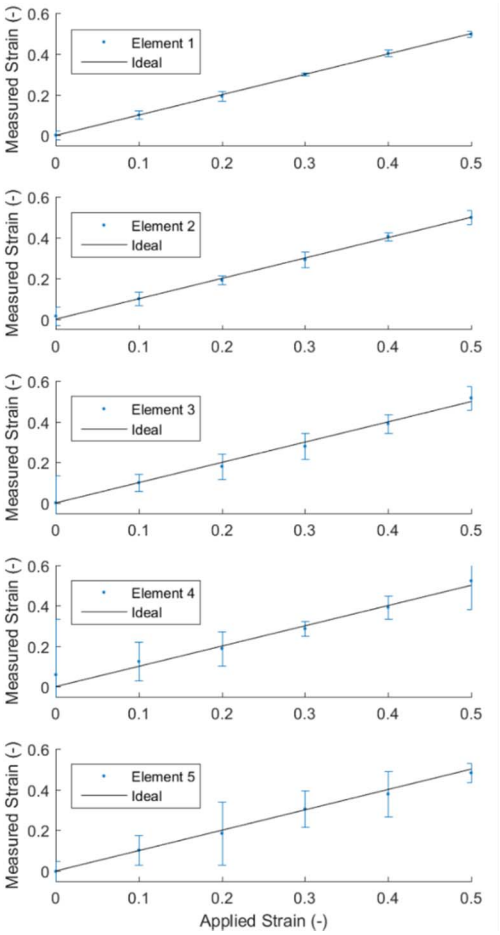


Fig. 3. Regression results of the trained artificial neural network. The plots show the reconstructed strain as points, with an ideal curve shown as a black line. Error bars represent 95% confidence intervals. Data shown represent 100 loading conditions generated using a Latin hypercube design. Individual tests include simultaneous loading of all elements with randomly assigned strain values.

As shown in Fig. 2, the response of the sensor to strain is not a simple function. We found that an artificial neural network (ANN) was required to obtain accurate reconstruction of the strain field. In order to train the ANN, we generated 100 test conditions using a Latin hypercube experimental design. Instead of considering the entire impedance spectrum, we limited our samples to 10 logarithmically spaced frequencies between 15.9kHz and 1.59MHz, simulating the capabilities of a physical, on-board measurement system. The impedance results from the finite element simulation for all 100 conditions at the 10 sample frequencies were used to train the ANN. 70 conditions were used for training, 15 for validation, and 15 to compute the performance. We used MATLAB's Neural Network Toolbox (MATLAB 2016a, NNT 9.0).

As a sensitivity study for the parameters of the ANN, we evaluated changes to the number of nodes in the hidden layer (3,5,7,10,15,20) and the number of frequencies (3,5,10,20,50,100). On average, we observed an order-of-magnitude improvement between 5 and 10 frequencies, but only marginal improvement beyond 10 frequencies. At 10 frequencies, we found significant improvement up to 10 nodes, but no significant improvement beyond that point. Because of this, we selected 10 nodes and 10 frequencies as our nominal ANN configuration.

Once trained, we used the ANN, with 10 frequencies and 10 hidden nodes, to reconstruct the strain in our simulated loading conditions. The reconstruction of the 100 loading conditions used to train the ANN are shown in Fig. 3. Testing with an additional set of conditions showed slightly higher errors. In Fig. 3, we show the reconstructed strain by element, although the strains were applied across all elements simultaneously in the test. The plots show that Element 1, which is closest to the electrical interface, has the lowest error and best fit across all values of applied strain. Moving away from the interface, Elements 2 through 5 have progressively larger error values. The increasing error is due to the decreasing change in magnitude of the impedance at elements further away from the interface, as shown in Fig. 2, coupled with the fact that strains are being applied to all elements at once. The strain approximations at distal elements show increasing error because the signal is overwhelmed by the signal from proximal elements. Through this evaluation, we determined that it is possible to use an ANN to uniquely reconstruct the spatial distribution of strain state in a capacitive sensor through a single interface.

## III. Conclusion

In this paper we have demonstrated a frequency-based method for measuring distributed strains in a deformable capacitive sensor. Our approach utilizes an electrode with finite resistance, which can be realized in practice using conductive elastomer composites. The method we have demonstrated can be used to reduce the number of individual sensors required to measure the distributed strains found in deformable systems, such as soft robots and wearable devices. This in turn improves the manufacturability of these devices, decreases the number of interfaces required, and thereby increases the overall reliability of the deformable system.

## IV. Acknowedgment

This work is partially supported under the NASA Early Career Faculty Program, Space Technology Research Grants Program (NNX14AO52G). ELW and MCY are supported by the NSF Graduate Research Fellowship (DGE-1333468).

## References

[1] D. Rus and M. T. Tolley, “Design, fabrication and control of soft robots,” Nature, vol. 521, no. 7553, pp. 467–475, May 2015.

[2] J. C. Case, E. L. White, and R. K. Kramer, “Sensor enabled closed-loop bending control of soft beams,” Smart Materials and Structures, vol. 25, no. 4, p. 045018, Apr. 2016.

[3] B. O'Brien, T. Gisby, I.A. Anderson. “Stretch sensors for human body motion,” Proc. SPIE 9056, Electroactive Polymer Actuators and Devices (EAPAD) 2014, 905618, Mar. 8, 2014.

[4] D. Xu, A. Tairych, and I. A. Anderson, “Where the rubber meets the hand: Unlocking the sensing potential of dielectric elastomers,” J. Polym. Sci. Part B: Polym. Phys., vol. 54, no. 4, pp. 465–472, Feb. 2016.

[5] D. Xu, A. Tairych, and I. A. Anderson, “Stretch not flex: programmable rubber keyboard,” Smart Mater. Struct.., vol. 25, p. 015012, Jan. 2016.

[6] A. Tairych, I.A. Anderson, “Distributed sensing: multiple capacitive stretch sensors on a single channel,” Proc. SPIE 10163, Electroactive Polymer Actuators and Devices (EAPAD) 2017, 1016306, Apr 17, 2017.

[7] E. L. White, M. C. Yuen, J. C. Case, and R. K. Kramer, “Low-cost, facile, and scalable manufacturing of capacitive sensors for soft systems,” Advanced Materials Technologies *(in press)*